Simultaneous Multi-Frequency Phase-Coded Microwave Signal Generation at Six Different Frequencies Using a DP-BPSK Modulator

Yang Chen, *Member, IEEE*, and Jianping Yao, *Fellow, IEEE, Fellow, OSA*

***Abstract*—An approach to the generation of a multi-frequency phase-coded microwave signal at six different microwave carrier frequencies using a laser diode and a dual-polarization binary phase-shift keying (DP-BPSK) modulator is proposed and experimentally demonstrated. The key component in the proposed system is the DP-BPSK modulator, which consists of two dual-drive Mach–Zehnder modulators (DD-MZMs) that are driven by a binary coding signal and a microwave reference signal. By controlling the bias points of the DD-MZMs, and the power of the coding signal and the microwave reference signal, phase-coded microwave signals at six different frequencies are generated at the output of a photodetector. An experiment is performed. A multi-frequency phase-coded microwave signal at six different carrier frequencies in a frequency range from 1 to 19.5 GHz is generated. The performance in terms of phase recovery accuracy and pulse compression capability is evaluated. The interferences between different channels are also evaluated and no significant interferences are observed.**

***Index Terms*—Microwave photonics, multiband radar, phase coding, photonic signal generation, pulse compression.**

I. Introduction

PHASE-CODED microwave signal is one of the microwave waveforms that are widely used in modern radar systems for pulse compression [1], [2]. A phase-coded microwave signal is usually generated in the electrical domain using an electronic circuit. However, with the rapid development of radar systems, new requirements for phase-coded microwave signals have emerged, such as higher frequency, wider frequency tunable range, and broader bandwidth. These requirements are difficult to fulfil using conventional electrical generation methods. Microwave photonics, taking advantages of the wide bandwidth and high operating frequency offered by photonics, is a solution to these problems [3]–[5]. In the past few years, numerous techniques based on microwave photonics for phase-coded microwave signal generation have been proposed.

A phase-coded microwave signal can be generated using free-space optics. The key advantage of using free-space optics is its high reconfigurability, which can enable reconfigurable waveform generation. However, a free-space optics based system is usually lossy and bulky [6]. Pure fiber-optics based approaches have been proposed to avoid the problems existing in a free-space optics based system. For example, a phase-coded microwave signal can be generated based on fiber-optics based optical spectrum shaping and frequency-to-time mapping [7]. However, the time duration of the generated waveform is very short due to the limited dispersion employed for frequency-to-time mapping, which makes the waveform have a small time bandwidth product (TBWP). Optical external modulation is a simple and effective solution to generate a phase-coded microwave signal with a long time duration [8]–[11]. With the rapid development of radar systems, phase-coded microwave signals are desired to be generated at an even higher frequency and wider bandwidth for applications such as high-resolution microwave imaging. Photonic-assisted phase-coded microwave signal generation at a higher frequency based on frequency multiplication has been researched and demonstrated recently [12]–[14]. However, in the approaches reported in [12]–[14], only a single frequency phase-coded microwave signal is generated. A radar that operates at multiple frequency bands may be more resilient to electromagnetic interferences. In addition, different frequencies for a radar system may have very different observation capability [15]–[17]. Therefore, it is highly desirable that a multiband radar system, which can observe targets using a multiband signal at different frequency bands, is employed to overcome the problems encountered in a single-frequency radar system and to enhance the observation capabilities [15], [16].

As early as in 1960s, National Aeronautics and Space Administration began to support studies on multiband radar systems [17]. To allow multiband operation of a radar system, we can make full use of different observation characteristics of radar signals at different frequency bands. However, if the multiband operation is achieved simply using multiple radar systems in different frequency bands, the system becomes extremely complex and costly. One solution is to integrate different functions of multiple radar systems at different frequency bands into a

Manuscript received November 13, 2018; revised February 1, 2019; accepted February 22, 2019. Date of publication February 27, 2019; date of current version April 17, 2019. This work was supported in part by the Natural Sciences and Engineering Research Council of Canada, in part by the National Natural Science Foundation of China under Grant 61601297, in part by the Open Fund of IPOC (BUPT), and in part by the Fundamental Research Funds for the Central Universities. *(Corresponding author: Yang Chen.)*

Y. Chen is with the Shanghai Key Laboratory of Multidimensional Information Processing, East China Normal University, Shanghai 200241, China, and also with the Microwave Photonics Research Laboratory, School of Electrical Engineering and Computer Science, University of Ottawa, Ottawa, ON K1N 6N5, Canada (e-mail: ychen@ce.ecnu.edu.cn).

J. Yao is with the Microwave Photonics Research Laboratory, School of Electrical Engineering and Computer Science, University of Ottawa, Ottawa, ON K1N 6N5, Canada (e-mail: jpyao@uottawa.ca).

Color versions of one or more of the figures in this paper are available online at http://ieeexplore.ieee.org.

Digital Object Identifier 10.1109/JLT.2019.2901924

single radar system. To do so, a key step is to generate a multi-band radar signal. A few approaches have been proposed recently. One method is to up-convert a phase-coded intermediate frequency signal to the RF bands at multiple frequencies using a mode-locked laser [18]. However, the phase coding process is still implemented in the electrical domain. In [19], [20], photonic phase coders with simultaneous multi-frequency phase coding were proposed using a multi-wavelength laser source. The structures of the two methods are simple and phase-coded microwave signals at multiple frequencies can be generated simultaneously. However, in the experimental demonstration, a multiband signal with only two frequencies were demonstrated. In addition, the use of a multi-wavelength laser source would increase the cost of the system. Furthermore, it is difficult to control the power of each frequency component individually unless the power of each individual wavelength of the multi-wavelength laser source can be controlled independently.

In this paper, we propose an approach to generate a multi-frequency phase-coded microwave signal at six frequencies using a single wavelength laser diode (LD) and a dual-polarization binary phase-shift keying (DP-BPSK) modulator. The key component of the system is the DP-BPSK modulator, which consists of two dual-drive Mach–Zehnder modulators (DD-MZMs). By biasing the DD-MZMs at specific bias points, and by controlling the power of the driving coding signals and the microwave reference signals, a multi-frequency phase-coded microwave signal at six different microwave carrier frequencies can be generated at the same power level. To the best of our knowledge, this is the first time that a photonic-assisted multiband phase-coded microwave signal at six carrier frequencies is generated. Compared with the previous work for multi-frequency phase-coded microwave signal generation, the proposed scheme is simpler as no multi-wavelength laser source is needed. A proof-of-concept experiment is performed. Simultaneous generation of a multi-frequency phase-coded microwave signal at six different carrier frequencies in a frequency range from 1 to 19.5 GHz is achieved. The performance in terms of phase recovery accuracy and pulse compression capability is evaluated. The interferences between the different channels are also evaluated and no significant interference is observed.

II. Principle

Fig. 1 shows the schematic diagram of the proposed multi-frequency phase-coded microwave signal generator. A continuous-wave (CW) light wave generated from an LD is injected into a DP-BPSK modulator, which consists of a 3-dB optical coupler, two DD-MZMs (DD-MZM1 and DD-MZM2), a 90° polarization rotator (PR), and a polarization beam combiner (PBC). For each DD-MZM, a microwave reference signal and a coding signal are applied to the DD-MZM via the two RF ports. The polarization state of the optical signal from the lower DD-MZM is rotated by 90° via the PR, and then combined with the optical signal from the upper DD-MZM at the PBC. The optical signal from the DP-BPSK modulator is sent to a PD, where a multi-frequency phase-coded microwave signal is generated.

Assuming the optical signal from the LD is $E_0(t)$, the microwave signal and the coding signal applied to DD-MZM1

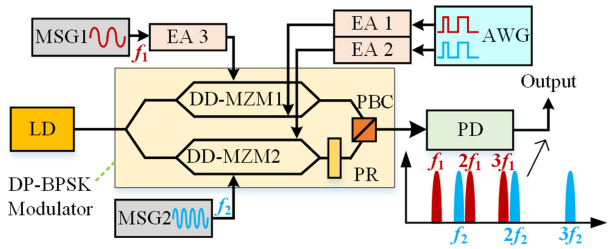

Fig. 1. Schematic diagram of the proposed multi-frequency phase-coded microwave signal generator. LD, laser diode; DP-BPSK modulator, dual-polarization binary phase-shift keying modulator; DD-MZM, dual-drive Mach–Zehnder modulators; PBC, polarization beam combiner; PR, 90° polarization rotator; MSG, microwave signal generator; AWG, arbitrary waveform generator; EA, electrical amplifier; PD, photodetector.

are $V_{r1}\cos(\omega_1 t)$ and $V_{c1}s_1(t)$, and the microwave signal and the coding signal applied to DD-MZM2 are $V_{r2}\cos(\omega_2 t)$ and $V_{c2}s_2(t)$, the optical signal at the output of the DP-BPSK modulator can be expressed as

$$\begin{bmatrix} E_x(t) \\ E_y(t) \end{bmatrix} = \frac{\sqrt{2}}{4}\alpha E_0(t)\begin{bmatrix} \exp(jm_1\cos\omega_1 t) + \exp(j\delta_1 s_1(t) + j\varphi_1) \\ \exp(jm_2\cos\omega_2 t) + \exp(j\delta_2 s_2(t) + j\varphi_2) \end{bmatrix}, \quad (1)$$

where α and V_π are the insertion loss and the half-wave voltage of the modulator, V_{r1} and V_{r2} are the amplitudes, ω_1 and ω_2 are the angular frequencies of the two microwave signals, respectively, V_{c1} and V_{c2} are the amplitudes of the coding signals $s_1(t)$ and $s_2(t)$, respectively, $m_1 = \pi V_{r1}/V_\pi$, $m_2 = \pi V_{r2}/V_\pi$, $\delta_1 = \pi V_{c1}/V_\pi$, $\delta_2 = \pi V_{c2}/V_\pi$, and φ_1 and φ_2 are the phase shifts introduced by the bias voltages of the two DD-MZMs.

When the optical signal from the DP-BPSK modulator is detected at the PD, the photocurrent at the output of the PD is given by

$$i(t) = \frac{1}{4}\alpha^2 R E_0^2 [2 + \cos(m_1\cos\omega_1 t - \delta_1 s_1(t) - \varphi_1) + \cos(m_2\cos\omega_2 t - \delta_2 s_2(t) - \varphi_2)], \quad (2)$$

where R is the responsivity of the PD, and E_0 is the amplitude of the optical signal from the LD.

If $\delta_1 = \delta_2 = \pi$, $s_1(t)$ and $s_2(t)$ are both unipolar sequences (0, 1), and $a_1(t)$ and $a_2(t)$ are the corresponding bipolar sequences (1, −1), (2) can be written as

$$\begin{aligned} i(t) &= \frac{1}{4}\alpha^2 R E_0^2 \{2 + a_1(t)\cos(m_1\cos\omega_1 t - \varphi_1) + a_2(t)\cos(m_2\cos\omega_2 t - \varphi_2)\} \\ &= \frac{1}{4}\alpha^2 R E_0^2 \left\{2 + a_1(t)\left[J_0(m_1)\cos\varphi_1 + 2\cos\varphi_1\sum_{n=1}^{\infty}(-1)^n J_{2n}(m_1)\cos 2n\omega_1 t\right.\right. \end{aligned}$$

$$
\begin{aligned}
&- 2\sin\varphi_1 \sum_{n=1}^{\infty} (-1)^n J_{2n-1}(m_1)\cos(2n-1)\omega_1 t\Bigg] \cdot \\
&+ a_2(t)\Bigg[J_0(m_2)\cos\varphi_2 \\
&+ 2\cos\varphi_2 \sum_{n=1}^{\infty} (-1)^n J_{2n}(m_2)\cos 2n\omega_2 t \\
&- 2\sin\varphi_2 \sum_{n=1}^{\infty} (-1)^n J_{2n-1}(m_2)\cos(2n-1)\omega_2 t\Bigg]\Bigg\} \qquad (3)
\end{aligned}
$$

It can be seen from (3) that multiple binary phase-coded microwave signals are generated at frequencies that are integral multiples of the frequencies of the two input microwave reference signals in addition to two baseband components. The amplitude of each frequency component is jointly determined by the amplitude of the microwave reference signal and the bias point of the modulator. We can control the amplitude of the microwave reference signal and the bias point of the modulator to generate different multi-frequency phase-coded microwave signal.

Specifically, a six-frequency phase-coded microwave signal with identical power can be generated when the following conditions are satisfied,

$$
\begin{cases}
J_1(m_1)\sin\varphi_1 = J_3(m_1)\sin\varphi_1 = \pm J_2(m_1)\cos\varphi_1 \\
J_1(m_2)\sin\varphi_2 = J_3(m_2)\sin\varphi_2 = \pm J_2(m_2)\cos\varphi_2
\end{cases} . \qquad (4)
$$

By solving the equations above, we get $m_1 = m_2 = 3.054$, $\varphi_1 = \varphi_2 = 0.991$ or -0.991. Under this condition, phase-coded microwave signals at ω_1, ω_2, $2\omega_1$, $2\omega_2$, $3\omega_1$ and $3\omega_2$ are simultaneously generated with an identical signal power. The sequences carried by the carriers at ω_1, $2\omega_1$ and $3\omega_1$ are determined by the coding signal $s_1(t)$, whereas the sequences carried by the carriers at ω_2, $2\omega_2$ and $3\omega_2$ are determined by the coding signal $s_2(t)$. In addition, when (4) is satisfied, the signal generation efficiency at each carrier frequency, which is defined as the power ratio of the generated phase-coded microwave signal to the input microwave reference signal, can be expressed as

$$
\eta = \frac{\pi^2 \alpha^4 R^2 E_0^4 J_1^2(m_1)\sin^2\varphi_1}{4m_1^2 V_\pi^2}. \qquad (5)
$$

III. Experimental Results

An experiment is carried out based on the setup shown in Fig. 1. An 8-dBm CW light wave centered at 1552.722 nm from an LD (Anritsu MG9638A) is sent to the DP-BPSK modulator (Fujitsu FTM 7980EDA) with a 3-dB bandwidth of about 20 GHz. Two binary coding signals generated from an arbitrary waveform generator (AWG, Agilent AWG7102) are amplified by two electrical amplifiers (EAs, Multilink, MTC5515) with each having a gain of 23 dB, and then applied to the DP-BPSK modulator via two RF ports. Two microwave reference signals generated from two microwave signal generators (MSG1, Agilent E8364A, MSG2, Agilent E8254A), are also applied to the DP-BPSK modulator via two other RF ports. The microwave signal from MSG1 is amplified by an EA (Multilink, MTC5515) because the maximum output power of MSG1 is limited to 8 dBm. The optical signal from the DP-BPSK modulator is then sent to the PD (in the experiment, two PDs are used, Nortel PP-10 G having a bandwidth of 10 GHz with a preamplifier and New Focus Model 1414 having a bandwidth of 25 GHz). The generated signal is monitored by a real-time oscilloscope (OSC, Agilent DSO-X 93204A), and its spectrum is measured by an electrical spectrum analyzer (ESA, Agilent E4448A).

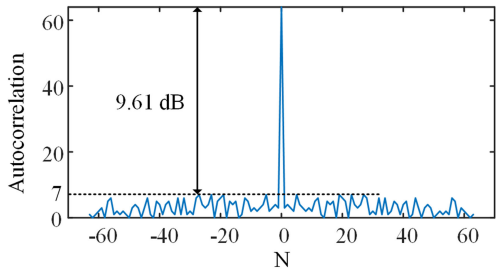

Fig. 2. Autocorrelation of the selected 64-bit binary sequence.

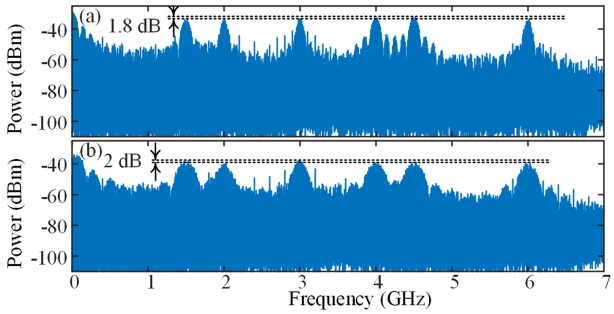

Fig. 3. Electrical spectra of the generated multi-frequency phase-coded microwave signals with coding speed of (a) 100 Mbps, (b) 200 Mbps, when the two microwave reference signals are 1.5 and 2 GHz.

In the experiment, the two coding signals are the same and are generated from the AWG. The coding signal is selected to be a 64-bit binary sequence, with a code pattern of "1111001100001000011001100010101000000101001001000 110100111110001". To get a better pulse compression performance, the coding signal is selected to have a high peak-to-sidelobe ratio (PSR). Fig. 2 shows the autocorrelation of the selected coding sequence. As can be seen, the PSR is 9.61 dB. The theoretical PSR of this coding sequence is better than most reported results using 64-bit random sequence as the coding sequence.

Then, the generation of the multi-frequency phase-coded microwave signal is evaluated. In the experiment, the frequencies of the two microwave reference signals applied to the modulator are set at 1.5 and 2 GHz, and the data rate of the coding signal is set at 100 or 200 Mbps. The PD used in this study has a bandwidth of 10 GHz. The electrical spectra of the generated phase-coded microwave signals at two data rates of 100 or 200 Mbps are shown in Fig. 3. It can be seen that phase-coded microwave signals are generated at six different frequencies that are integral multiples of 1.5 or 2 GHz. The coding speed is limited to 250 Mbps because the minimum frequency spacing

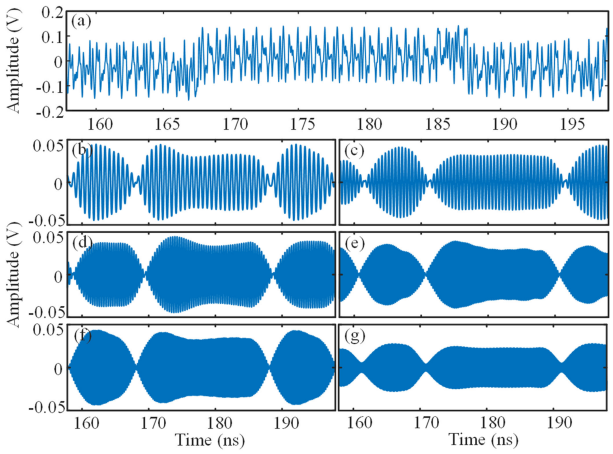

Fig. 4. A section of the waveform of the generated multi-frequency phase-coded microwave signal (a), and the corresponding extracted waveform with carrier frequencies of (b) 1.5 GHz, (c) 2 GHz, (d) 3 GHz, (e) 4 GHz, (f) 4.5 GHz, and (g) 6 GHz.

between the six frequencies are 500 MHz. In this study, we use 200 Mbps as the maximum coding speed. As can be seen from Fig. 3, the power difference between the six frequencies is less than 2 dB.

Fig. 4(a) shows a section of the waveform from the generated multi-frequency phase-coded microwave signal when the coding sequence is 100 Mbps. Since the six phase-coded microwave signals are superimposed in the time domain, to be able to see each of the six signals, a digital filter with a center frequency tuned at each of the six frequencies is employed to select one signal at one time. Fig. 4(b)–(g) shows the waveforms of the six phase-coded signals. It can be seen that the six waveforms are well recovered with different carrier frequencies and obvious phase jumps.

Then, the phase information from each of the six waveforms is extracted, which is done by Hilbert transform. The results are shown as dotted lines in the left figures of Fig. 5. The recovered phase information is in consistent with the selected binary coding sequence, and approximate π phase jumps between adjacent "0" and "1" can be clearly observed. The pulse compression performance of the generated phase-coded microwave signals is also verified as shown in the right figures of Fig. 5. The dotted lines in these figures show the theoretical autocorrelation. As can be seen the experimental measurements demonstrate good agreement with the theoretical results. The PSRs of the six phase-coded microwave signals are 9.21, 9.27, 8.59, 8.59, 9.17, and 9.31 dB, which are very close to the theoretical PSR of the selected coding sequence shown in Fig. 2. The insets show the zoom-in views of the autocorrelation peaks. The full-width at half-maximums (FWHMs) of the autocorrelation peaks are 10.42, 11.51, 12.46, 11.50, 10.54 and 11.45 ns, corresponding to pulse compression ratios (PCRs) of 61.42, 55.60, 51.36, 55.65, 61.67 and 55.89. When the bit rate of the coding sequence is 200 Mbps, similar results are obtained.

Then, the frequencies of the microwave reference signals are set at 2 and 2.5 GHz, and 1 and 2.5 GHz to evaluate the frequency tunability of the proposed system, with the electrical spectra shown in Fig. 6. Phase-coded microwave signals are

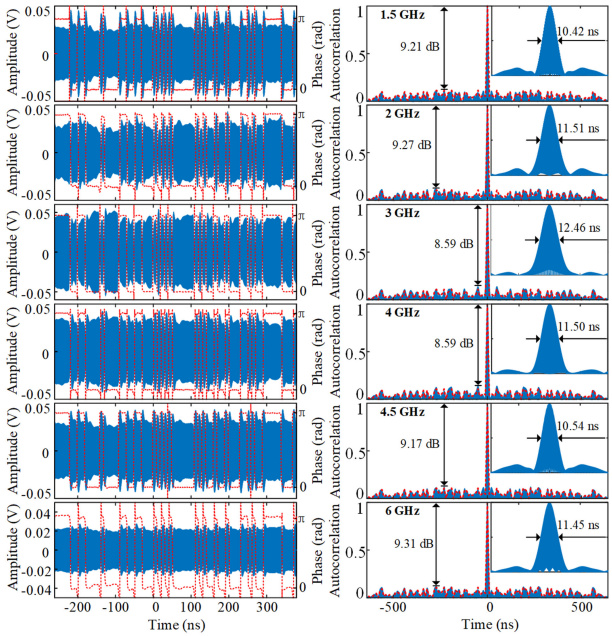

Fig. 5. Temporal waveforms and the recovered phase information (left), and the corresponding pulse compression performance (right) when carrier frequencies are from 1.5 to 6 GHz. The dotted line in the right figures are the theoretical autocorrelation of the coding sequence used in the experiment, and the insets of the right figures show the zoom-in views of the autocorrelation peaks.

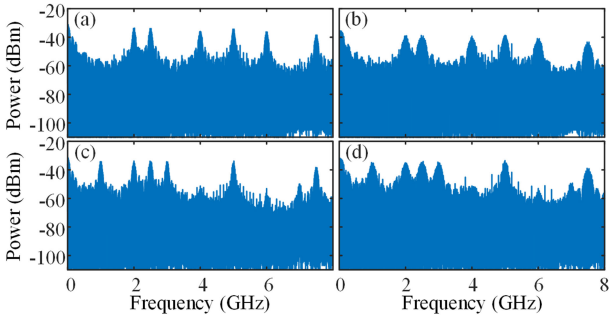

Fig. 6. Electrical spectra of the generated multi-frequency phase-coded microwave signals with coding speed of (a) 100 Mbps, (b) 200 Mbps, when the two microwave reference signals are 2 and 2.5 GHz; electrical spectra of the generated multi-frequency phase-coded microwave signals with coding speed of (c) 100 Mbps, (d) 200 Mbps, when the two microwave reference signals are 1 and 2.5 GHz.

simultaneously generated at six different frequencies that are integral multiples of the two microwave reference signals. Some intermodulation components are observed in Fig. 6(c) and (d). However, they are more than 13 dB suppressed, and will be eliminated after the mixed spectrum is sliced by six digital filters. It is also found that the power consistency of the six frequencies is not as good as that shown in Fig. 3, which is mainly caused by the relatively low-power highest frequency component. The highest frequency shown in Fig. 6 is increased compared with that shown in Fig. 3, so its power is correspondingly attenuated, which is associated with the frequency response of the PD.

The phase recovery accuracy and pulse compression capability are also evaluated. We only show the results of the waveform corresponding to the spectrum shown in Fig. 6(d) here. Hilbert transform is used to extract the phase information from one period of each waveform at different frequencies from 1 to

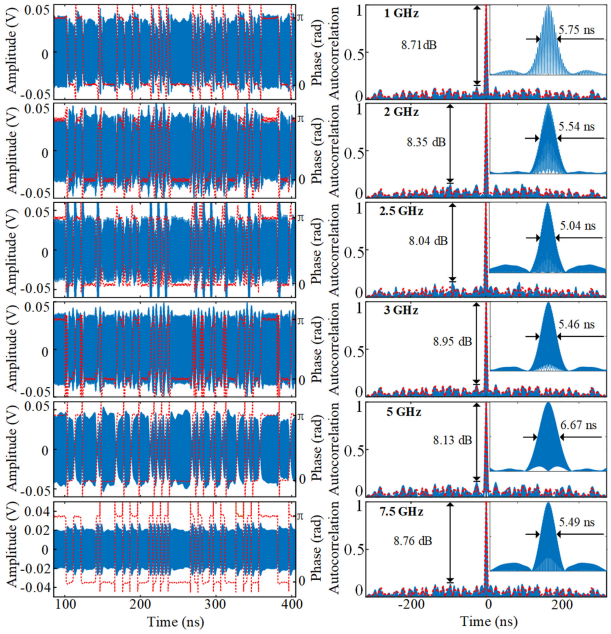

Fig. 7. Temporal waveforms and the recovered phase information (left), and the corresponding pulse compression performance (right) when carrier frequencies are from 1 to 7.5 GHz. The dotted line in the right figures are the theoretical autocorrelation of the coding sequence used in the experiment, and the insets of the right figures show the zoom-in views of the autocorrelation peaks.

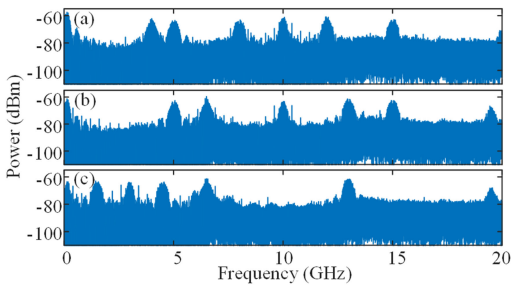

Fig. 8. Electrical spectra of the generated multi-frequency phase-coded microwave signals with coding speed of 400 Mbps, when the two microwave reference signals are (a) 4 and 5 GHz, (b) 5 and 6.5 GHsz, (c) 1.5 and 6.5 GHz.

7.5 GHz, with the results shown in dotted lines in the left figures of Fig. 7. The recovered phase information is in consistent with the selected binary coding sequence, and approximate π phase jumps between adjacent "0" and "1" can be clearly observed. The pulse compression performance is also evaluated, as shown in the right figures of Fig. 7. The dotted lines in these figures show the theoretical autocorrelation of the coding sequence. The experimental measurements also show very good consistency with the theoretical results. The PSRs of the six phase-coded microwave signals are 8.71, 8.35, 8.04, 8.95, 8.13, and 8.76 dB, and the corresponding PCRs are 55.65, 57.76, 63.49, 58.61, 47.98 and 58.29.

The frequency of the generated multi-frequency phase-coded microwave signal can be further increased by increasing the frequencies of the microwave reference signals. Fig. 8 shows the spectra of the generated multi-frequency phase-coded microwave signals when the frequencies of the microwave reference signals are 4 and 5 GHz, 5 and 6.5 GHz, and 1.5 and

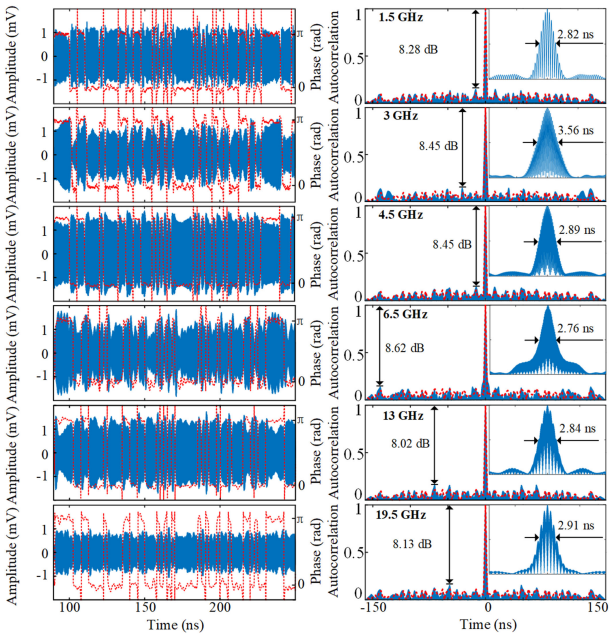

Fig. 9. Temporal waveforms and the recovered phase information (left), and the corresponding pulse compression performance (right) when carrier frequencies are from 1.5 to 19.5 GHz. The dotted line in the right figures are the theoretical autocorrelation of the coding sequence used in the experiment, and the insets of the right figures show the zoom-in views of the autocorrelation peaks.

6.5 GHz, respectively. As can be seen, six different frequency components are simultaneously generated. The PD used in this experiment has a bandwidth of 25 GHz, so the power of the highest frequency is relatively lower if it is close to 25 GHz. In addition, the 25-GHz PD does not integrate preamplifier in it, so the power of the generated signals is lower than those shown in Figs. 3 and 6.

The phase recovery and pulse compression performance are also verified. We only show the results of the waveform corresponding to the spectrum shown in Fig. 8(c) here. The left figures of Fig. 9 show the temporal waveforms and the corresponding recovered phase information of the six different phase-coded microwave signals from 1.5 to 19.5 GHz. It can be seen that the recovered phase changes according to the selected binary coding sequence, and the phase jumps between adjacent "0" and "1" are approximately π. The pulse compression performance of the phase-coded microwave signals is also verified, as shown in the right figures of Fig. 9. Compressed narrow pulses are obtained. The PSRs for the phase-coded microwave signals from 1.5 to 19.5 GHz are 8.28, 8.45, 8.45, 8.62, 8.02, and 8.13 dB, and the corresponding PCRs are 56.74, 44.94, 55.36, 57.97, 56.34, and 54.98.

In the experiments, the mixed phase-coded microwave signals from the PD is post-processed by Matlab to distinguish each frequency component by using digital filters with different central frequencies. From the performance in terms of the phase recovery accuracy and pulse compression capability obtained from the experiments, no significant crosstalk is observed between the desired frequency component and other frequency components. We can consider the very small crosstalks from

other phase-coded microwave signals as another contribution to the total noise of the desired phase-coded microwave signal in addition to the conventional thermal noise, shot noise and relative intensity noise, which may reduce the signal-to-noise ratio of a generated phase-coded microwave signal. The highest frequency of the phase-coded microwave signals generated in the experiment is 19.5 GHz, which is mainly limited by the bandwidth of the OSC used in the experiment. A typical DP-BPSK modulator has a 3-dB modulation bandwidth of 20 GHz, which means the highest frequency of the generated multi-frequency phase-coded microwave signal can reach 60 GHz. The 6-dB modulation bandwidth of a DP-BPSK modulator is larger than 40 GHz. If microwave reference signals with even higher frequency are applied, phase-coded microwave signals higher than 120 GHz can be generated at the cost of an additional 3-dB optical power loss, which can be compensated by an optical amplifier in the optical domain. From (4), we know that the modulation indices of the system should be properly set to ensure that the power of the generated six phase-coded microwave signals is equal. Under this condition, the signal generation efficiency expressed in (5) is related to the insertion loss and the half-wave voltage of the modulator, the responsivity of the PD, and the power of the input optical signal. To increase the signal generation efficiency, we can use a modulator with a small insertion loss and low half-wave voltage, increase the power of the input optical signal, or employ a PD with a high responsivity.

There is always a trade-off between the system complexity and the number of phase-coded microwave signals that can be generated. The proposed technique provides a good solution to generate phase-coded microwave signals at six different frequencies using a relatively simple structure. As demonstrated in the theory, the six phase-coded microwave signals are divided into two groups. The frequency of each group is determined by one of the two microwave reference signals, and the sequence on each group is determined by one of the two coding signals. The proposed system can only generate phase-coded microwave signals with frequencies that are integral multiples of the frequencies of the two microwave reference signals, and with sequences that are associated with the two coding signals applied to the modulator. In the experimental demonstration, several pairs of microwave reference signals are chosen to verify the performance of the system. Actually, in practical applications, the frequencies of the two microwave reference signals can be flexibly chosen. However, due to the six frequencies are integral multiples of the frequencies of the two microwave reference signals, it should be avoided that the first three harmonics of one microwave reference signal is close to those of the other microwave reference signal to ensure that phase-coded microwave signals at six different frequencies can be generated without spectrum aliasing. The minimum spacing between these six frequencies determines the maximum bandwidth of the generated phase-coded microwave signals.

Fig. 10 shows the relationship between the bandwidth and a typical frequency distribution of the multi-frequency phase-coded microwave signal. As can be seen from Fig. 10(a), when the minimum frequency spacing is fixed, the maximum bandwidth of the phase-coded microwave signal is identical to the minimum frequency spacing if the two groups of phase-coded

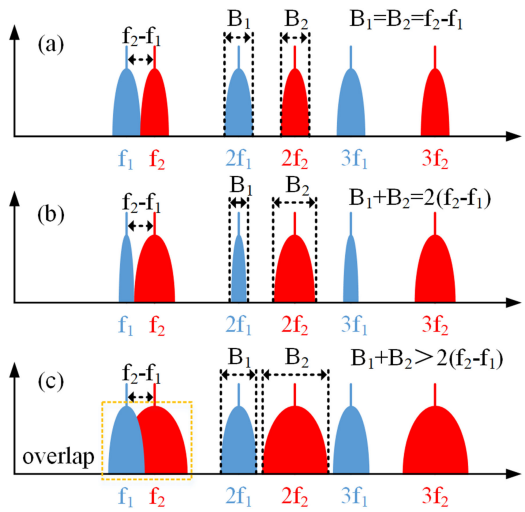

Fig. 10. Schematic diagram of the relationship between the bandwidth and a typical frequency distribution of the multi-frequency phase-coded microwave signals.

microwave signals are coded using coding sequence with the same data rate. However, we can also increase the bandwidth of one group of the six phase-coded microwave signals and decrease that of the other group to make the system more flexible. The only thing should be noticed to guarantee six usable phase-coded microwave signals is that the sum of the bandwidths of the two groups of phase-coded microwave signals should be equal to twice the minimum frequency spacing, as shown in Fig. 10(b). If phase-coded microwave signals with even larger bandwidth is required, we can still increase the bandwidth of the two groups of phase-coded microwave signals as shown in Fig. 10(c) at the cost of reducing the number of phase-coded microwave signals that can be used. In this case, the phase-coded microwave signals centered at f_1 and f_2 overlap each other, so we can only use the phase-coded microwave signals at other four frequencies.

For the detection of the multi-frequency phase-coded microwave signals, a solution is to use an optical-frequency-comb-based frequency down-conversion method, to work jointly with analog-to-digital conversion and digital signal processing [15]. The number of carriers in the multi-frequency phase-coded microwave signals is six, which is larger than that reported in Ref. [15]. However, the frequency down-conversion and detection of the six-carrier multi-frequency phase-coded microwave signal generated in this paper can also be implemented using an optical frequency comb.

IV. Conclusion

In summary, we have theoretically and experimentally investigated a photonic-assisted multi-frequency phase-coded microwave signal generator based on an LD and a DP-BPSK modulator. The key component in the system was a DP-BPSK modulator consisting of two DD-MZMs that were both driven by a binary coding signal and a microwave reference signal. By controlling the bias points of the DD-MZMs, and the power of the coding signals and the microwave reference signals, a multi-frequency phase-coded microwave signal at six different

microwave carrier frequencies were generated at the same power level. An experiment was performed. Phase-coded microwave signals at carrier frequencies that were integral multiples of 1.5 and 2 GHz, 1 and 2.5 GHz, 1.5 and 6.5 GHz were generated, with the performance in terms of phase recovery accuracy and pulse compression capability evaluated. The generated phase-coded microwave signals can achieve a PSR of more than 8 dB, and a PCR of more than 55. The proposed technique provides a new way to generate multi-frequency phase-coded microwave signals, which may find applications in multiband radar systems.

REFERENCES

[1] M. Skolnik, "Role of radar in microwaves," *IEEE Trans. Microw. Theory Techn.*, vol. 50, no. 3, pp. 625–632, Mar. 2002.

[2] M. Cohen, "Pulse compression in radar systems," in *Principles of Modern Radar*. New York, NY, USA: Springer, 1987, pp. 465–501.

[3] P. Ghelfi *et al.*, "A fully photonics-based coherent radar system," *Nature*, vol. 507, no. 7492, pp. 341–345, Mar. 2014.

[4] J. Yao, "Microwave photonics," *J. Lightw. Technol.*, vol. 27, no. 3, pp. 314–335, Feb. 2009.

[5] X. Zou, B. Lu, W. Pan, L. Yan, A. Stöhr, and J. Yao, "Photonics for microwave measurements," *Laser Photon. Rev.*, vol. 10, no. 5, pp, 711–734, Sep. 2016.

[6] J. McKinney, D. Leaird, and A. Weiner, "Millimeter-wave arbitrary waveform generation with a direct space-to-time pulse shaper," *Opt. Lett.*, vol. 27, no. 5, pp. 1345–1347, Aug. 2002.

[7] A. Weiner, "Ultrafast optical pulse shaping: A tutorial review," *Opt. Commun.*, vol. 284, no. 15, pp. 3669–3692, Jul. 2011.

[8] Z. Li, W. Li, H. Chi, X. Zhang, and J. Yao, "Photonic generation of phase-coded microwave signal with large frequency tunability," *IEEE Photon. Technol. Lett.*, vol. 23, no. 11, pp. 712–714, Jun. 2011.

[9] Z. Tang, T. Zhang, F. Zhang, and S. Pan, "Photonic generation of a phase-coded microwave signal based on a single dual-drive Mach–Zehnder modulator," *Opt. Lett.*, vol. 38, no. 24, pp. 5365–5368, Dec. 2013.

[10] Y. Chen, A. Wen, Y. Chen, and X. Wu, "Photonic generation of binary and quaternary phase-coded microwave waveforms with an ultra-wide frequency tunable range," *Opt. Express*, vol. 22, no. 13, pp. 15618–15625, Jun. 2014.

[11] P. Ghelfi, F. Scotti, F. Laghezza, and A. Bogoni, "Photonic generation of phase-modulated RF signals for pulse compression techniques in coherent radars," *J. Lightw. Technol.*, vol. 30, no. 11, pp. 1638–1644, Jun. 2012.

[12] Y. Chen, A. Wen, and J. Yao, "Photonic generation of frequency tunable binary phase-coded microwave waveforms," *IEEE Photon. Technol. Lett.*, vol. 25, no. 23, pp. 2319–2322, Dec. 2013.

[13] Y. Zhang, F. Zhang, and S. Pan, "Generation of frequency-multiplied and phase-coded signal using an optical polarization division multiplexing modulator," *IEEE Trans. Microw. Theory Techn.*, vol. 65, no. 2, pp. 651–660, Feb. 2017

[14] Y. Chen and S. Pan, "Photonic generation of tunable frequency-multiplied phase-coded microwave waveforms," *IEEE Photon. Technol. Lett.*, vol. 30, no. 13, pp. 1230–1233, Jul. 2018.

[15] P. Ghelfi, F. Laghezza, F. Scotti, D. Onori, and A. Bogoni, "Photonics for radars operating on multiple coherent bands," *J. Lightw. Technol.*, vol. 34, no. 2, pp. 500–507, Jan. 2016.

[16] M. Imhoff *et al.*, "BioSAR: An inexpensive airborne VHF multiband SAR system for vegetation biomass measurement," *IEEE Trans. Geosci. Remote Sens.*, vol. 38, no. 3, pp. 1458–1462, May 2000.

[17] L. Dellwig, "A geoscience evaluation of multifrequency radar imagery of the pisgah crater area, California," 1968. [Online]. Available: https://ntrs.nasa.gov/archive/nasa/casi.ntrs.nasa.gov/19690023260.pdf

[18] P. Ghelfi, F. Scotti, F. Laghezza, and A. Bogoni, "Phase coding of RF pulses in photonics-aided frequency-agile coherent radar systems," *IEEE J. Quantum Electron.*, vol. 48, no. 9, pp. 1151–1157, Sep. 2012.

[19] D. Zhu, W. Xu, Z. Wei, and S. Pan, "Multi-frequency phase-coded microwave signal generation based on polarization modulation and balanced detection," *Opt. Lett.*, vol. 41, no. 1, pp. 107–110, Jan. 2016.

[20] D. Wu *et al.*, "Photonic generation of multi-frequency phase-coded microwave signal based on a dual-output Mach-Zehnder modulator and balanced detection," *Opt. Express*, vol. 25, no. 13, pp. 14516–14523, Jun. 2017.

Yang Chen (S'12–M'17) received the B.E. degree in telecommunications engineering, and the Ph.D. degree in communication and information system, both from Xidian University, Xi'an, China, in 2009 and 2015, respectively.

He joined the School of Information Science and Technology, East China Normal University, Shanghai, China, in 2017, where he is currently a Research Professor. From 2012 to 2014, he was a joint-training Ph.D. student with the Microwave Photonics Research Laboratory, School of Electrical Engineering and Computer Science, University of Ottawa, Ottawa, ON, Canada. His current research interests include microwave photonics, optoelectronic oscillators, radio-over-fiber techniques, and optical communications.

Jianping Yao (M'99–SM'01–F'12) received the Ph.D. degree in electrical engineering from the Université de Toulon et du Var, Toulon, France, in December 1997. He is a Distinguished University Professor and a University Research Chair with the School of Electrical Engineering and Computer Science, University of Ottawa, Ottawa, ON, Canada. From 1998 to 2001, he was with the School of Electrical and Electronic Engineering, Nanyang Technological University, Singapore, as an Assistant Professor. In December 2001, he joined the School of Electrical Engineering and Computer Science, University of Ottawa, as an Assistant Professor, where he was promoted to an Associate Professor in May 2003, and a Full Professor in May 2006. He was appointed as the University Research Chair in Microwave Photonics in 2007. In June 2016, he was conferred the title of Distinguished University Professor of the University of Ottawa. From July 2007 to June 2010 and July 2013 to June 2016, he served as the Director of the Ottawa-Carleton Institute for Electrical and Computer Engineering. He has authored or coauthored more than 560 research papers including more than 330 papers in peer-reviewed journals and more than 230 papers in conference proceedings.

Prof. Yao is the Editor-in-Chief of IEEE PHOTONICS TECHNOLOGY LETTERS, a Topical Editor of *Optics Letters*, an Associate Editor of *Science Bulletin*, a Steering Committee Member of JOURNAL OF LIGHTWAVE TECHNOLOGY, and an Advisory Editorial Board member of *Optics Communications*. He was a Guest Editor of a Focus Issue on *Microwave Photonics in Optics Express* in 2013, a Lead-Editor of a Feature Issue on *Microwave Photonics in Photonics Research* in 2014, and a Guest Editor of a special issue on Microwave Photonics in IEEE JOURNAL OF LIGHTWAVE TECHNOLOGY in 2018. He currently serves as the Chair of the IEEE Photonics Ottawa Chapter, and is the Technical Committee Chair of IEEE MTT-3 Microwave Photonics. He was a member of the European Research Council Consolidator Grant Panel in 2016, the Qualitative Evaluation Panel in 2017, and a member of the National Science Foundation Career Awards Panel in 2016. He has also served as a Chair of a number of international conferences, symposia, and workshops, including the Vice Technical Program Committee (TPC) Chair of the 2007 IEEE Topical Meeting on Microwave Photonics, the TPC Co-Chair of the 2009 and 2010 Asia-Pacific Microwave Photonics Conference, the TPC Chair of the high-speed and broadband wireless technologies subcommittee of the IEEE Radio Wireless Symposium 2009–2012, the TPC Chair of the microwave photonics subcommittee of the IEEE Photonics Society Annual Meeting 2009, the TPC Chair of the 2010 IEEE Topical Meeting on Microwave Photonics, the General Co-Chair of the 2011 IEEE Topical Meeting on Microwave Photonics, the TPC Co-Chair of the 2014 IEEE Topical Meetings on Microwave Photonics, and the General Co-Chair of the 2015 and 2017 IEEE Topical Meeting on Microwave Photonics. He has also served as a committee member for a number of international conferences, such as IPC, OFC, BGPP, and MWP. He was the recipient of the 2005 International Creative Research Award of the University of Ottawa, the 2007 George S. Glinski Award for Excellence in Research, and the Natural Sciences and Engineering Research Council of Canada Discovery Accelerator Supplements Award in 2008. He was selected to receive an inaugural OSA Outstanding Reviewer Award in 2012 and was one of the top ten reviewers of JOURNAL OF LIGHTWAVE TECHNOLOGY 2015–2016. He was an IEEE MTT-S Distinguished Microwave Lecturer for 2013–2015. He was the recipient of the Award for Excellence in Research 2017–2018 of the University of Ottawa. He is a registered Professional Engineer of Ontario. He is a Fellow of the Optical Society of America, the Canadian Academy of Engineering, and the Royal Society of Canada.